INTERNATIONAL JOURNAL OF ADAPTIVE CONTROL AND SIGNAL PROCESSING
Int. J. Adapt. Control Signal Process. 2010; **24**:261–274
Published online 15 May 2009 in Wiley InterScience (www.interscience.wiley.com). DOI: 10.1002/acs.1128

Indirect adaptive control of a class of marine vehicles

Yannick Morel and Alexander Leonessa*, †

Mechanical Engineering Department, Virginia Polytechnic Institute and State University, Blacksburg, VA 24061-0238, U.S.A.

SUMMARY

A nonlinear adaptive framework for bounded-error tracking control of a class of non-minimum phase marine vehicles is presented. The control algorithm relies on a special set of tracking errors to achieve satisfactory tracking performance while guaranteeing stable internal dynamics. First, the design of a model-based nonlinear control law, guaranteeing asymptotic stability of the error dynamics, is presented. This control algorithm solves the tracking problem for the considered class of marine vehicles, assuming full knowledge of the system model. Then, the analysis of the zero-dynamics is carried out, which illustrates the efficacy of the chosen set of tracking errors in stabilizing the internal dynamics. Finally, an indirect adaptive technique, relying on a partial state predictor, is used to address parametric uncertainties in the model. The resulting adaptive control algorithm guarantees Lyapunov stability of the errors and parameter estimates, as well as asymptotic convergence of the errors to zero. Numerical simulations illustrate the performance of the adaptive algorithm. Copyright © 2009 John Wiley & Sons, Ltd.

Received 23 April 2008; Revised 19 December 2008; Accepted 5 March 2009

KEY WORDS: adaptive nonlinear control; adaptive tracking; nonlinear uncertain systems; indirect multi-input/multi-output adaptive control; autonomous marine vehicles

1. INTRODUCTION

Autonomous marine vehicles (AMVs) are used for a wide range of tasks, completion of which either requires or greatly benefits from a high-performance positioning and navigation system. Research on motion control of AMVs has received considerable attention from the community over the past decades [1–10]. However, the tracking problem for one of the most commonly encountered class of marine vehicles (i.e. marine vehicles equipped with a fixed thruster and a rudder) is rarely considered. Notable exceptions include [2], which contains simplifying assumptions removing relevant dynamic behaviors.

The lack of a systematic study of this particular problem can be partially explained by the difficulty in solving the full motion control problem for an AMV equipped with a fixed thruster and a rudder. Mathematical models describing the dynamical behavior of such vehicles are nonlinear, feature a significant degree of uncertainty, potentially both parametric and structural, are underactuated, and the internal dynamics resulting from this underactuation are not necessarily stable [8].

Nevertheless, a number of control algorithms designed for underactuated marine vehicles can be found in the literature (for instance, [5–9]). In [5], the tracking control problem for a surface ship equipped with a pair of propellers is addressed. However, the desired trajectory is limited to straight lines and circles.

*Correspondence to: Alexander Leonessa, Mechanical Engineering Department, Virginia Polytechnic Institute and State University, Blacksburg, VA 24061-0238, U.S.A.
†E-mail: leonessa@vt.edu

In [6], the authors consider the same type of propulsion system as in [5], and an additional state estimator is used to address uncertainties on state measurements. In [7], a similar twin propellers scenario is considered, and external disturbances, such as ocean currents, are accounted for. In [8], a controller for an underactuated AMV equipped with a propeller and a side thruster is designed. The corresponding vehicle's model is fairly similar to that of a vehicle with a thruster and rudder, as it includes a coupling between sway force and yawing moment. The controller also handles constant and slow varying external perturbations.

Issues resulting from parametric uncertainties in a vehicle's model can be addressed using adaptive control techniques. In [10], the authors present an adaptive control framework relying on a particular error variable corresponding to the angle between the vehicle's longitudinal axis and the direction of the vehicle's desired position. The resulting controller solves the regulation problem for an underactuated AMV. The introduction of this relative orientation is progressively spreading through the literature. It can be found in [11] and, more recently, in [12].

The control of underactuated marine vehicles with an unstable zero-dynamics (or underactuated non-minimum phase marine vehicles) is rarely treated. Two notable exceptions are [11, 13]. The result in [11] is limited to way-point maneuvering and requires full knowledge of the system's model. The control algorithm introduced in [13] solves the tracking control problem for uncertain systems, relying on a neural network-based approach similar to the classical direct adaptive techniques. However, the control algorithm is rather complex and relies on approximations of the time derivatives of a number of variables involved in the backstepping design [14]. While these approximations allow to avoid the 'explosion of terms' issue inherent to backstepping procedures [15], they might negatively affect transient performance.

To solve the trajectory tracking problem for the considered class of systems, we use a backstepping procedure [14]; however, special care has to be taken in choosing the tracking errors since this choice affects the stability properties of the internal dynamics. More specifically, an inadequate choice of tracking errors can lead to an unstable behavior of the internal dynamics [8, 16]. To address this issue, we build upon the approach introduced in [10] and develop a control strategy similar to that presented in [13]. In particular, we choose the tracking errors as the distance between the current and desired position, and relative direction of this desired position. The resulting behavior of the internal dynamics is investigated by assessing the stability of the zero-dynamics.

The mathematical model of the system that we consider features parametric uncertainties. Such lack of knowledge is often addressed using direct adaptive techniques. However, for our choice of tracking errors, when using a backstepping technique [16], the unknown parameters will appear nonlinearly in the control command. Thus, we are not able to rely on the certainty equivalence principle to derive a direct adaptive algorithm. This nonlinear parametrization can be addressed using Dynamic Surface Control [15], as seen in [13]. In this case, filters are designed in addition to the backstepping procedure, which not only simplify the expressions involved in the derivations, but also lead to a control command linear in the uncertain parameters. The choice of time constants for these filters is critical. Indeed, large time constants lead to a smooth command, but can add delays and result in poor transient performance. Alternately, small time constants can improve the transient, but might also lead to a noisy command. To remedy this situation and avoid the tradeoff between the smoothness of the command and transient performance, we propose an indirect adaptive approach. The algorithm relies on a partial state predictor (similar to that used in [17]) to determine the appropriate command to the system, as opposed to relying on the uncertain portion of the actual model. As described in the following sections, the use of this technique gives rise to a new issue. Indeed, the closed form of the control command includes the inverse of a matrix that is function of the estimates. To avoid singularity of this matrix, we use a projection algorithm [18] to constrain the estimates to appropriate values.

In Section 2, we present the considered three degree of freedom model and the reference system. Section 3 describes the control strategy and introduces a control law guaranteeing asymptotic stability of the tracking errors, assuming full knowledge of the system's model,

DOI: 10.1002/acs

for motion of a class of marine vehicles in three degrees of freedom. Section 4 assesses the stability of the zero-dynamics. Using a state predictor, Section 5 introduces an indirect adaptive control law, which guarantees Lyapunov stability and convergence of the tracking errors in spite of parametric uncertainties, and details the projection algorithm used to avoid singularity of the command. Results of numerical simulations are presented in Section 6. Finally, Section 7 concludes this paper.

2. SYSTEM DYNAMICS

The behavior of an AMV in the horizontal plane can be described using the following model [19]:

$$\dot{\eta}(t) = J(\eta(t))v(t), \quad \eta(0)=\eta_0, \ \ t\geqslant 0 \tag{1}$$

$$\dot{v}(t) = -M^{-1}(D(v(t))+C(v(t)))v(t) - M^{-1}g(\eta(t)) + M^{-1}B\tau(t), \quad v(0)=v_0 \tag{2}$$

where the position of the system is described by $\eta(t)\triangleq[x(t)\ y(t)\ \psi(t)]^{\mathrm{T}}\in\mathbb{R}^2\times(-\pi,\pi],\ t\geqslant 0$, with $x(t)$ and $y(t)$ representing the vehicle's position in an inertial frame of arbitrary origin, and $\psi(t)$ is the yaw angle, measured between the inertial x-axis and the longitudinal axis of symmetry of the vehicle. The velocity is represented in the body-fixed frame of reference and denoted with $v(t)\triangleq[u(t)\ v(t)\ r(t)]^{\mathrm{T}}\in\mathbb{R}^3,\ t\geqslant 0$, where $u(t)$ and $v(t)$ represent the surge and sway velocity, respectively, and $r(t)$ is the angular velocity in yaw. In addition, the rotation matrix $J(\psi)$, inertia matrix M, damping matrix $D(v)$, and Coriolis matrix $C(v)$ are of the form [19]

$$J(\eta)=\begin{bmatrix}\cos(\psi) & -\sin(\psi) & 0\\ \sin(\psi) & \cos(\psi) & 0\\ 0 & 0 & 1\end{bmatrix} \tag{3}$$

$$M=\begin{bmatrix}m_1 & 0 & 0\\ 0 & m_2 & m_{23}\\ 0 & m_{23} & m_3\end{bmatrix}$$

$$D(v)=\begin{bmatrix}d_{l1}+d_{q1}|u| & 0 & 0\\ 0 & d_{l2}+d_{q2}|v| & d_{l23}+d_{q23}|r|\\ 0 & d_{l23}+d_{q23}|v| & d_{l3}+d_{q3}|r|\end{bmatrix} \tag{4}$$

$$C(v)=\begin{bmatrix}0 & 0 & -m_2v-m_{23}r\\ 0 & 0 & m_1u\\ m_2v+m_{23}r & -m_1u & 0\end{bmatrix} \tag{5}$$

The vector of restoring forces and moments will be assumed to be the three-by-one zero matrix $0_{3\times 1}$. Finally, the input matrix B is given by

$$B\triangleq\begin{bmatrix}1 & 0\\ 0 & -1/l\\ 0 & 1\end{bmatrix} \tag{6}$$

where $l>0$ represents the arm of the sway force generated by the rudder with respect to the center of gravity of the vehicle, and the control input is $\tau(t)\triangleq[\tau_1(t)\ \ \tau_2(t)]^{\mathrm{T}}\in\mathbb{R}^2,\ t\geqslant 0$.

Note that (1) and (2) only represent an approximation of an actual marine vehicle's dynamical behavior. In particular, the damping matrix only provides a crude approximation of the effect of linear skin friction on the vehicle's hull and quadratic drag. However, in the literature, this model is commonly assumed to provide a reasonable approximation of the system's dynamics, and overall strikes an agreeable balance between accuracy and complexity. Note that the input matrix B characterizes the type of propulsion system featured on the vehicle. The form of B given by (6) accommodates either a fixed thruster with a rudder or a vectored thruster.

The dynamics (2) can be expressed in a more compact form by factorizing the uncertain parameters,

$$\dot{v}(t)=\Theta_1^*\varphi_1(v(t))+\Theta_2^*\tau(t), \quad v(0)=v_0, \quad t\geqslant 0 \tag{7}$$

DOI: 10.1002/acs

with

$$\Theta_1^* \triangleq -M^{-1}\begin{bmatrix} d_{l1} & 0 & 0 & d_{q1} & 0 & 0 & 0 & 0 & -m_2 & -m_{23} \\ 0 & d_{l2} & d_{l23} & 0 & d_{q2} & d_{q23} & 0 & m_1 & 0 & 0 \\ 0 & d_{l23} & d_{l3} & 0 & d_{q23} & d_{q3} & m_2-m_1 & m_{23} & 0 & 0 \end{bmatrix} \quad (8)$$

$$\Theta_2^* \triangleq M^{-1}B = \begin{bmatrix} \theta_{21}^* & 0 \\ 0 & \theta_{22}^* \\ 0 & \theta_{23}^* \end{bmatrix}, \quad \varphi_1(v) \triangleq [v^{\mathrm{T}} \ \ |u|u \ \ |v|v \ \ |r|r \ \ uv \ \ ur \ \ vr \ \ r^2]^{\mathrm{T}} \quad (9)$$

The control algorithms presented in the next sections utilize a model reference framework. More specifically, the trajectory we want the system to track is generated by the reference system

$$\begin{bmatrix} \dot{x}_{r1}(t) \\ \dot{x}_{r2}(t) \end{bmatrix} = \begin{bmatrix} 0_{2\times 2} & I_2 \\ -\omega_0^2 & -2\zeta\omega_0 \end{bmatrix} \begin{bmatrix} x_{r1}(t) \\ x_{r2}(t) \end{bmatrix} + \begin{bmatrix} 0_{2\times 2} \\ \omega_0^2 \end{bmatrix} r_s(t) \quad (10)$$

$$\begin{bmatrix} x_{r1}(0) \\ x_{r2}(0) \end{bmatrix} = \begin{bmatrix} x_{r10} \\ x_{r20} \end{bmatrix}, \quad t \geqslant 0$$

where $x_{r1}(t),\ x_{r2}(t) \in \mathbb{R}^2,\ t \geqslant 0, x_r(t) \triangleq [x_{r1}(t)^{\mathrm{T}}\ x_{r2}(t)^{\mathrm{T}}]^{\mathrm{T}}$, $t \geqslant 0$, represents the state of the reference system, and $r_s(t) \in \mathbb{R}^2,\ t \geqslant 0$, denotes the reference input. Furthermore, I_2 is the 2-dimensional identity matrix, the matrices $\omega_0,\ \zeta \in \mathbb{R}^{2\times 2}$ are positive definite, $\omega_0^2 \triangleq \omega_0\omega_0$, and we define

$$A_r \triangleq \begin{bmatrix} 0_{2\times 2} & I_2 \\ -\omega_0^2 & -2\zeta\omega_0 \end{bmatrix} \quad (11)$$

3. NONLINEAR CONTROL ALGORITHM

We consider the following tracking errors:

$$e_d(\eta, x_{r1}) \triangleq \|x_{r1} - [x \ \ y]^{\mathrm{T}}\| \quad (12)$$

$$\beta(\eta, x_{r1}) \triangleq \mathrm{atan2}(x_{r12} - y, x_{r11} - x) - \psi \quad (13)$$

where x_{r11} and x_{r12} are the components of x_{r1}, such that $x_{r1} \triangleq [x_{r11}\ x_{r12}]^{\mathrm{T}}$, $\mathrm{atan2}(\alpha_1, \alpha_2) \triangleq \arg(\alpha_1 + \mathrm{i}\alpha_2)$, for all $(\alpha_1, \alpha_2) \in \mathbb{R}^2 \setminus (0,0)$, and $\arg(z)$ is the argument of $z \in \mathbb{C}$, such that $\arg(z) = \varphi$ whenever $z = |z|\mathrm{e}^{\mathrm{i}\varphi}$, with $\varphi \in (-\pi, \pi]$ and $\mathrm{i} \triangleq \sqrt{-1}$.

The errors defined in (12) and (13) are of particular geometric significance. More specifically, $e_d(\cdot) \in \mathbb{R}^+$ represents the distance between system and reference position, while $\beta(\cdot) \in (-\pi, \pi]$ corresponds to the angle from the longitudinal, u-axis of the body-fixed frame to the direction from system to the reference position. Note that, when $e_d(\cdot) = 0,\ \beta(\cdot)$ is undefined, ($\mathrm{atan2}(\alpha_1, \alpha_2)$ is undefined for $\alpha_1 = \alpha_2 = 0$).

The control objective is bounded-error tracking. More specifically, we will attempt to obtain $(e_d(t), \beta(t)) \to (a, 0)$ as $t \to \infty$, with $a > 0$. We group these errors in the vector $e_1(\eta, x_{r1}) \triangleq [e_d(\eta, x_{r1})\ \ \beta(\eta, x_{r1})]^{\mathrm{T}}$ and obtain the following time derivative of $e_1(\eta(t), x_{r1}(t))$:

$$\dot{e}_1(t) = \begin{bmatrix} 1 & 0 \\ 0 & 1/e_d(t) \end{bmatrix} J_s^{\mathrm{T}}(\beta(t))\varphi_0(\eta(t), v(t), x_r(t))$$

$$e_1(0) = e_1(\eta_0, x_{r10}), \quad t \geqslant 0 \quad (14)$$

where $J_s(\cdot)$ denotes the upper left, two-by-two block of (3), that is

$$J_s(\cdot) \triangleq \begin{bmatrix} \cos(\cdot) & -\sin(\cdot) \\ \sin(\cdot) & \cos(\cdot) \end{bmatrix} \quad (15)$$

and

$$\varphi_0(\eta, v, x_r) \triangleq J_s^{\mathrm{T}}(\psi)x_{r2} + B_e(e_1(\eta, x_{r1}))v$$

$$B_e(e_1) \triangleq \begin{bmatrix} -1 & 0 & e_d\sin(\beta) \\ 0 & -1 & -e_d\cos(\beta) \end{bmatrix} \quad (16)$$

DOI: 10.1002/acs

Since $\dot{e}_1(t),\ t\geqslant 0$, is not an explicit function of $\tau(t),\ t\geqslant 0$, we are unable to use (14) to directly determine the command law. However, we observe that $\tau(t),\ t\geqslant 0$, directly affects the rate of change of $v(t),\ t\geqslant 0$ (see (7)). Furthermore, $\varphi_0(\eta(t), v(t), x_r(t))$, $t\geqslant 0$, is an explicit function of $v(t),\ t\geqslant 0$, and directly affects $\dot{e}_1(t),\ t\geqslant 0$ (see (14)). Because of this particular structure, the control problem can be solved using a backstepping technique [14]. More specifically, considering the error dynamics described by (14), we introduce the following Lyapunov function candidate:

$$V_0(e_1)\triangleq e_d\tan^2\left(\frac{\beta}{2}\right)+\frac{1}{2e_d}(e_d-a)^2$$
$$e_d>0,\quad \beta\in(-\pi,\pi) \tag{17}$$

Note that $V_0(e_1)$ is a positive-definite function of e_d-a and β, but is not defined for $\beta=\pi$. The time derivative of (17) is of the form

$$\dot{V}_0(t)=\gamma^{\mathrm{T}}(e_1(t))J_s^{\mathrm{T}}(\beta(t))\varphi_0(\eta(t),v(t),x_r(t))$$
$$t\geqslant 0 \tag{18}$$

where $\gamma(e_1)\triangleq[\tan^2(\beta/2)+(e_d^2-a^2)/2e_d^2\ \sin(\beta/2)/\cos^3(\beta/2)]^{\mathrm{T}}$. Treating $\varphi_0(\cdot)$ as a virtual command [14], we define the velocity error

$$e_2(t)\triangleq \varphi_0(\eta(t),v(t),x_r(t))$$
$$+e_d(t)J_s(\beta(t))G_1\gamma(e_1(t)),\quad t\geqslant 0 \tag{19}$$

where $G_1>0$, such that

$$\dot{V}_0(t)=-e_d(t)\gamma^{\mathrm{T}}(e_1(t))G_1\gamma(e_1(t))$$
$$+e_2^{\mathrm{T}}(t)J_s(\beta(t))\gamma(e_1(t)),\quad t\geqslant 0 \tag{20}$$

Note that

$$\dot{e}_2(t)=J_s^{\mathrm{T}}(\psi(t))(-\omega_0^2x_{r1}(t)+(r(t)S-2\zeta\omega_0)x_{r2}(t)$$
$$+\omega_0^2r_s(t))+r(t)S\varphi_0(t)+\varphi_2(e_1(t),e_2(t))$$
$$+B_e(e_1(t))\Theta_1^*\varphi_1(v(t))+B_e(e_1(t))\Theta_2^*\tau(t)$$
$$e_2(0)=e_2(\eta_0,v_0,x_{r0}),\quad t\geqslant 0 \tag{21}$$

where $x_{r0}\triangleq[x_{r10}^{\mathrm{T}}\ \ x_{r20}^{\mathrm{T}}]^{\mathrm{T}}$, and

$$\varphi_2(e_1,e_2)\triangleq J_s(\beta)G_1\left(\begin{bmatrix}\frac{a^2}{e_d^2} & \frac{\sin(\beta/2)}{\cos^3(\beta/2)}\\ 0 & \frac{2-\cos(\beta)}{2\cos^4(\beta/2)}\end{bmatrix}\right.$$
$$\left.+[\gamma(e_1)\ \tilde{G}\gamma(e_1)]\right)J_s^{\mathrm{T}}(\beta)$$
$$\times(e_2-e_dJ_s(\beta)G_1\gamma(e_1)) \tag{22}$$

with

$$S\triangleq\begin{bmatrix}0 & 1\\ -1 & 0\end{bmatrix},\quad \tilde{G}\triangleq G_1^{-1}S^{\mathrm{T}}G_1 \tag{23}$$

The following result builds upon the above Lyapunov function candidate (17) and velocity error (19), and presents a control law guaranteeing asymptotic stability of the error dynamics (14) and (21), which implies asymptotic convergence of $e_1(t),\ t\geqslant 0$, to $[a\ \ 0]^{\mathrm{T}}$, assuming knowledge of the uncertain parameters Θ_1^* and Θ_2^*.

Theorem 3.1
Consider the error dynamics given by (14) and (21), assume that $B_e(e_1(t))\Theta_2^*,\ t\geqslant 0$, is non-singular, and that $\beta(0)\neq\pi$. Then, the feedback control law

$$\tau^*(t)=(B_e(e_1(t))\Theta_2^*)^{-1}(-B_e(e_1(t))\Theta_1^*\varphi_1(v(t))$$
$$-J_s^{\mathrm{T}}(\psi(t))(-\omega_0^2x_{r1}(t)+(r(t)S-2\zeta\omega_0)x_{r2}(t)$$
$$+\omega_0^2r_s(t))-\varphi_2(e_1(t),\ e_2(t))-r(t)S\varphi_0(t)$$
$$-J_s(\beta(t))\gamma(e_1(t))-G_2e_2(t)),\quad t\geqslant 0 \tag{24}$$

guarantees that the solution $[e_d(t)\ \ \beta(t)]^{\mathrm{T}}\equiv[a\ \ 0]^{\mathrm{T}}$, $e_2(t)\equiv 0_{2\times 1},\ t\geqslant 0$, to (14) and (21), is asymptotically stable.

DOI: 10.1002/acs

Proof
Substituting (19) into (14), we obtain

$$\dot{e}_1(t) = \begin{bmatrix} 1 & 0 \\ 0 & 1/e_{\mathrm{d}}(t) \end{bmatrix} J_{\mathrm{s}}^{\mathrm{T}}(\beta(t)) e_2(t) - \begin{bmatrix} e_{\mathrm{d}}(t) & 0 \\ 0 & 1 \end{bmatrix} G_1 \gamma(e_1(t)), \quad t \geqslant 0 \tag{25}$$

Similarly, substituting the feedback control law (24) into (21) yields

$$\dot{e}_2(t) = -J_{\mathrm{s}}(\beta(t))\gamma(e_1(t)) - G_2 e_2(t), \quad t \geqslant 0 \tag{26}$$

Note that the closed-loop tracking error dynamics, given by (25)–(26), is autonomous. Next, consider the Lyapunov function candidate

$$V(e_1, e_2) \triangleq e_{\mathrm{d}} \tan^2\left(\frac{\beta}{2}\right) + \frac{1}{2e_{\mathrm{d}}}(e_{\mathrm{d}} - a)^2 + \frac{1}{2} e_2^{\mathrm{T}} e_2 \tag{27}$$

which is a positive definite function of $e_{\mathrm{d}} - a$, β, and e_2. The time derivative along the closed-loop trajectories of (25) and (26) is given by

$$\begin{aligned} \dot{V}(t) &= -e_{\mathrm{d}}(t)\gamma^{\mathrm{T}}(e_1(t)) G_1 \gamma(e_1(t)) + \gamma^{\mathrm{T}}(e_1(t)) J_{\mathrm{s}}^{\mathrm{T}}(\beta(t)) \\ &\quad \times e_2(t) - e_2^{\mathrm{T}}(t)(J_{\mathrm{s}}(\beta(t))\gamma(e_1(t)) + G_2 e_2(t)) \\ &= -e_{\mathrm{d}}(t)\gamma^{\mathrm{T}}(e_1(t)) G_1 \gamma(e_1(t)) \\ &\quad - e_2^{\mathrm{T}}(t) G_2 e_2(t), \quad t \geqslant 0 \end{aligned} \tag{28}$$

Since $e_{\mathrm{d}}\gamma^{\mathrm{T}}(e_1) G_1 \gamma(e_1)$ is a positive-definite function of $e_{\mathrm{d}} - a$ and β, it follows that $\dot{V}(t) < 0$, $t \geqslant 0$, and the solution $[e_{\mathrm{d}}(t) \ \beta(t)]^{\mathrm{T}} \equiv [a \ 0]^{\mathrm{T}}$, $e_2(t) \equiv 0_{2\times 1}$, $t \geqslant 0$, to the error dynamics given by (25) and (26) is asymptotically stable. □

Remark 3.1
For any point $(e_{10}, e_{20}) \in \mathscr{D}_e \triangleq \mathbb{R}^+ \times (-\pi, \pi) \times \mathbb{R}^2$, define $c \triangleq V(e_{10}, e_{20})$. Since $V(e_1, e_2) \to \infty$ whenever either $e_{\mathrm{d}} \to \infty$, $\|e_2\| \to \infty$, or e_1 approaches the boundaries of $\mathscr{D}_e$, it follows that $\Omega_c \triangleq \{(e_1, e_2) \in \mathscr{D}_e : V(e_1, e_2) \leqslant c\}$ is compact, as illustrated by Figure 1. Hence, the result in Theorem 3.1 holds for any initial condition in $\mathscr{D}_e$.

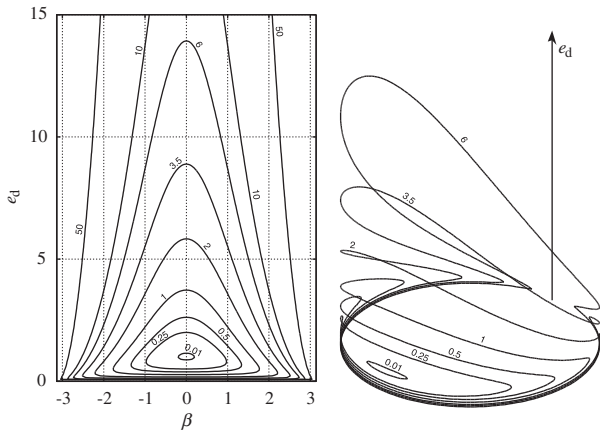

Figure 1. Level sets of $V(e_1, e_2)$ for $e_2 = 0$, represented in the plane (left) and on the cylinder (right).

Remark 3.2
In order to guarantee that the level sets of the Lyapunov function (27) are closed curves in the domain of definition, we did not consider the case $\beta = \pi$, which implies that the initial condition $x_{\mathrm{r}10}$ of the reference system, given by (10), cannot be chosen directly behind the initial position η_0 of the actual vehicle.

4. INTERNAL DYNAMICS ANALYSIS

The control law presented in the previous section is such that the tracking error $e_1(\eta, x_{\mathrm{r}1})$ asymptotically converges to $[a \ 0]^{\mathrm{T}}$. However, the stability analysis that led to the proof of Theorem 3.1 does not account for the behavior of the internal dynamics, which is essential in assessing the merit of the control approach.

4.1. Zero-dynamics

Consider the following change of coordinates:

$$\Phi(s) = \begin{bmatrix} \xi_1^1(s) \\ \xi_2^1(s) \\ \xi_1^2(s) \\ \xi_2^2(s) \\ \varsigma_1(s) \\ \varsigma_2(s) \end{bmatrix} \triangleq \begin{bmatrix} e_{\mathrm{d}}(s) \\ L_f e_{\mathrm{d}}(s) \\ \beta(s) \\ L_f \beta(s) \\ \psi \\ m_4 v + m_5 r \end{bmatrix} \tag{29}$$

DOI: 10.1002/acs

where $s \triangleq (\eta, v, x_r)$, $f(s) \triangleq [v^T J^T(\eta) \;\; \varphi_1^T(v)\Theta_1^{*T} \;\; x_r^T A_r^T]^T$, $m_4 \triangleq lm_2 + m_{23}$, $m_5 \triangleq m_3 + lm_{23}$, and $L_f h(s) \triangleq h'(s) f(s)$ denotes the Lie derivative of $h(s)$ with respect to $f(s)$. Note that $\Phi(\cdot)$ maps the six states (x, y, ψ, u, v, r) into six new states $(\xi_1^1, \xi_2^1, \xi_1^2, \xi_2^2, \varsigma_1, \varsigma_2)$, while $x_r \in \mathbb{R}^4$, for the purpose of this analysis, represents an exogenous signal. Computing $\Phi^{-1}(\cdot)$, we obtain

$$\eta(\xi, \varsigma, x_r) = [x_{r11} - \xi_1^1 \cos(\xi_1^2 - \varsigma_1) \;\; x_{r12} - \xi_1^1 \sin(\xi_1^2 - \varsigma_1) \;\; \varsigma_1]^T \tag{30}$$

$$v(\xi, \varsigma, x_r) = \frac{1}{m_6(\xi)} \begin{bmatrix} -m_6(\xi) & m_4 \xi_1^1 \sin(\xi_1^2) & \xi_1^1 \sin(\xi_1^2) \\ 0 & -m_5 & -\xi_1^1 \cos(\xi_1^2) \\ 0 & m_4 & 1 \end{bmatrix} \begin{bmatrix} \xi_2^1 \cos(\xi_1^2) - \xi_1^1 \xi_2^2 \sin(\xi_1^2) - x_{r21} \cos(\varsigma_1) - x_{r22} \sin(\varsigma_1) \\ \xi_2^1 \sin(\xi_1^2) + \xi_1^1 \xi_2^2 \cos(\xi_1^2) + x_{r21} \sin(\varsigma_1) - x_{r22} \cos(\varsigma_1) \\ \varsigma_2 \end{bmatrix} \tag{31}$$

where $\xi \triangleq [\xi_1^1 \;\; \xi_2^1 \;\; \xi_1^2 \;\; \xi_2^2]^T$, $\varsigma \triangleq [\varsigma_1 \;\; \varsigma_2]^T$, and $m_6(\xi) \triangleq m_5 - m_4 \xi_1^1 \cos(\xi_1^2)$.

Next, let $\mathscr{X}_0 \triangleq \{(\eta, v) : \Phi(s) = \xi_0\} \subset \mathbb{R}^6$, where $\xi_0 \triangleq [a \;\; 0 \;\; 0 \;\; 0]^T$. Note that when $(\eta, v) \in \mathscr{X}_0$, $\Phi^{-1} : (\xi, \varsigma, x_r) \to (\eta, v, x_r)$ is well defined if $\xi_1^1 \neq 0$ and $a \neq m_5/m_4$. The zero-dynamics is defined as the dynamics of the uncontrolled states $\varsigma_i(t)$, $t \geqslant 0$, $i = 1, 2$, when $\xi(t) \equiv \xi_0$, $t \geqslant 0$, and it is given by

$$\dot{\varsigma}_1(t) = \frac{1}{m_5 - am_4}(\varsigma_2(t) + m_4[\sin(\varsigma_1(t)) - \cos(\varsigma_1(t))] x_{2r}(t))$$

$$\varsigma_1(0) = \psi_0, \;\; t \geqslant 0 \tag{32}$$

$$\dot{\varsigma}_2(t) = [l \;\; 1](D_0(\xi_0, \varsigma(t)) + C_0(\xi_0, \varsigma(t))) \times [v(\xi_0, \varsigma(t)) \;\; r(\xi_0, \varsigma(t))]^T$$

$$\varsigma_2(0) = m_4 v_0 + m_5 r_0 \tag{33}$$

where

$$D_0(\xi_0, \varsigma) \triangleq \begin{bmatrix} d_{l2} + d_{q2}|v(\xi_0, \varsigma)| & d_{l23} + d_{q23}|r(\xi_0, \varsigma)| \\ d_{l23} + d_{q23}|v(\xi_0, \varsigma)| & d_{l3} + d_{q3}|r(\xi_0, \varsigma)| \end{bmatrix}, \quad C_0(\xi_0, \varsigma) \triangleq u(\xi_0, \varsigma) \begin{bmatrix} 0 & m_1 \\ m_2 - m_1 & m_{23} \end{bmatrix} \tag{34}$$

To illustrate the effect of the maximum allowable error $a > 0$ on the zero-dynamics, we will consider a simple reference trajectory with a constant x_{r2}. The motion of a marine vehicle along a straight line is a control problem of importance, especially in the context of way-point maneuvering [11]. The equilibrium configuration of interest for the zero-dynamics is as follows:

$$\varsigma_{1,eq} = \operatorname{atan2}(x_{r22}, x_{r21}) \tag{35}$$

$$\varsigma_{2,eq} = 0 \tag{36}$$

as it corresponds to the vehicle traveling along the straight desired trajectory with a positive velocity $u(t)$, $t \geqslant 0$. The corresponding linearization of (32) and (33) about that equilibrium configuration yields

$$\begin{bmatrix} \dot{\varsigma}_1(t) \\ \dot{\varsigma}_2(t) \end{bmatrix} = \begin{bmatrix} \left.\frac{\partial \dot{\varsigma}_1}{\partial \varsigma_1}\right|_{eq} & \left.\frac{\partial \dot{\varsigma}_1}{\partial \varsigma_2}\right|_{eq} \\ \left.\frac{\partial \dot{\varsigma}_2}{\partial \varsigma_1}\right|_{eq} & \left.\frac{\partial \dot{\varsigma}_2}{\partial \varsigma_2}\right|_{eq} \end{bmatrix} \begin{bmatrix} \varsigma_1(t) \\ \varsigma_2(t) \end{bmatrix}$$

$$\varsigma(0) = [\varsigma_1(0) \;\; \varsigma_1(0)]^T, \quad t \geqslant 0 \tag{37}$$

where

$$\left.\frac{\partial \dot{\varsigma}_1}{\partial \varsigma_1}\right|_{eq} = \frac{m_4 u_e}{m_5 - am_4}, \quad \left.\frac{\partial \dot{\varsigma}_1}{\partial \varsigma_2}\right|_{eq} = \frac{1}{m_5 - am_4} \tag{38}$$

DOI: 10.1002/acs

$$\left.\frac{\partial\dot{\varsigma}_2}{\partial\varsigma_1}\right|_{\text{eq}} = \frac{u_e}{m_5 - am_4}(m_4(ld_{l3}+d_{l23}) - m_5(ld_{l2}+d_{l23}) + u_e(m_4(lm_1+m_{23}) - m_5(m_2-m_1))) \quad (39)$$

$$\left.\frac{\partial\dot{\varsigma}_2}{\partial\varsigma_2}\right|_{\text{eq}} = \frac{1}{m_5 - am_4}(ld_{l3}+d_{l23} - a(ld_{l2}+d_{l23}) + u_e(m_1(l+a)+m_{23}-am_2)) \quad (40)$$

and $u_e \triangleq \sqrt{x_{r21}^2 + x_{r22}^2}$.

4.2. Minimum value of a

Studying the stability of the linear system (37), we obtain the range of values for a that would guarantee stability of the considered equilibrium point as a function of the various constant parameters characterizing the system's dynamics. However, given the complexity of the obtained expressions, we will limit ourselves to a numerical estimation of the range of a using the values of the aforementioned constant parameters corresponding to the Silent Quick Unmanned Intelligent Diver 2 (SQUID-2, [16]). The values used are the following:

$$M = \begin{bmatrix} 53.1748 & 0 & 0 \\ 0 & 87.4858 & 12.254 \\ 0 & 12.254 & 7.3346 \end{bmatrix} \quad (41)$$

$$D(v) = \begin{bmatrix} 6.855+8.246|u| & 0 & 0 \\ 0 & 25.094+48.329|v| & 10.668+14.649|r| \\ 0 & 10.668+14.649|v| & 4.002+7.331|r| \end{bmatrix} \quad (42)$$

and $l = 0.5$. In addition, we choose $u_e = 1$.

As seen in Figure 2, the eigenvalues of the state matrix display a singular behavior at $a_s = m_5/m_4 \simeq 0.1964$. For $a < a_s$, both eigenvalues λ_1 and λ_2 are positive and the considered equilibrium point is unstable. However, for $a > a_s$, the eigenvalues are strictly negative. As emphasized earlier, the introduction of the maximum allowable position error a is allowed to stabilize the zero-dynamics. Indeed, without this position error, the zero-dynamics equilibrium configuration of interest is unstable, while it becomes stable for $a > a_s$.

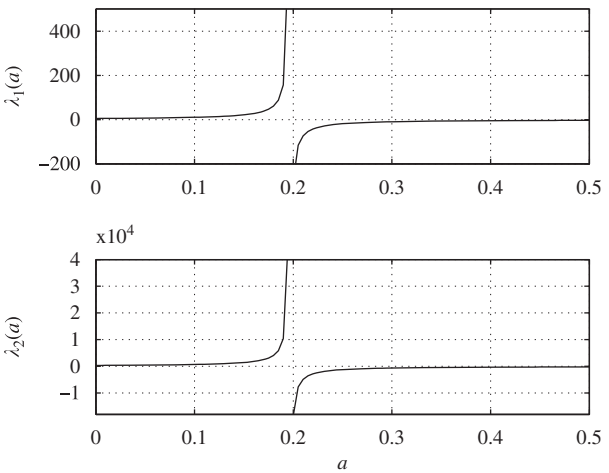

Figure 2. Eigenvalues of the Jacobian matrix in (37) versus a.

5. INDIRECT ADAPTIVE ALGORITHM

It is clear from (24) that, in order to compute the value of the command, knowledge of the exact values of Θ_1^* and Θ_2^* are required. Since this information is not necessarily available, it would appear desirable to obtain a control law only requiring estimates of these parameters. However, classical direct adaptive techniques rely on a linearly parameterized command (to allow the application of the equivalence certainty principle). In our case, the term $(B_e(e_1(t))\Theta_2^*)^{-1}$ is nonlinear in the

DOI: 10.1002/acs

uncertain parameters, which we will address using an indirect adaptive approach.

In particular, we will make use of the partial state predictor

$$\dot{\hat{v}}(t)=\Theta_1(t)\varphi_1(v(t))+\tau_d(t)\Theta_{2v}(t)+u_p(t)$$
$$\hat{v}(0)=v_0,\quad t\geqslant 0 \tag{43}$$

where $\Theta_1(t)\in\mathbb{R}^{3\times 10}$ and $\Theta_{2v}(t)\triangleq[\theta_{21}(t)\ \theta_{22}(t)\ \theta_{23}(t)]^{\mathrm{T}}\in\mathbb{R}^{3\times 1}$, $t\geqslant 0$, are estimates of Θ_1^* and $\Theta_{2v}^*\triangleq[\theta_{21}^*\ \theta_{22}^*\ \theta_{23}^*]^{\mathrm{T}}$, respectively, $\hat{v}(t)\triangleq[\hat{u}(t)\ \hat{v}(t)\ \hat{r}(t)]^{\mathrm{T}}$, $t\geqslant 0$, and $\tau_d(t)\triangleq\mathrm{diag}([\tau_1(t)\ \tau_2(t)\ \tau_2(t)])$, $t\geqslant 0$. The predictor signal $u_p(t)\in\mathbb{R}^3$, $t\geqslant 0$, will be designed to improve performance of the predictor, allowing (43) to emulate the dynamics in (2).

5.1. Adaptive control command

Consider the error

$$e_v(t)\triangleq v(t)-\hat{v}(t),\quad t\geqslant 0 \tag{44}$$

which reflects the difference between the vehicle's velocity and its estimate, provided by the state predictor (43). The time derivative of (44) is given by

$$\begin{aligned}\dot{e}_v(t)&=\Theta_1^*\varphi_1(v(t))+\Theta_2^*\tau(t)-\Theta_1(t)\varphi_1(v(t))\\&\quad-\Theta_2(t)\tau(t)-u_p(t)\\&=(\Theta_1^*-\Theta_1(t))\varphi_1(v(t))+\tau_d(t)(\Theta_{2v}^*-\Theta_{2v}(t))\\&\quad-u_p(t),\quad e_v(0)=v_0-\hat{v}_0,\quad t\geqslant 0\end{aligned} \tag{45}$$

We will now modify the velocity error defined by (19) so that the control algorithm relies on the fully known state predictor, instead of the actual system's dynamics, which are uncertain. To do so, we define the new velocity error

$$\begin{aligned}\hat{e}_2(t)&\triangleq\varphi_0(\eta(t),\hat{v}(t),x_r(t))\\&\quad+e_d(t)J_s(\beta(t))G_1\gamma(e_1(t)),\quad t\geqslant 0\end{aligned} \tag{46}$$

which is similar to (19), the only difference being its dependence upon $\hat{v}(t)$, $t\geqslant 0$, as opposed to $v(t)$, $t\geqslant 0$. Note that, using (16) and (44), we can rewrite (46) as

$$\begin{aligned}\hat{e}_2(t)&\triangleq\varphi_0(\eta(t),v(t),x_r(t))-B_e(e_1(t))e_v(t)\\&\quad+e_d(t)J_s(\beta(t))G_1\gamma(e_1(t)),\quad t\geqslant 0\end{aligned} \tag{47}$$

The time derivative of (46) is given by

$$\begin{aligned}\dot{\hat{e}}_2(t)&=J_s^{\mathrm{T}}(\psi(t))(-\omega_0^2x_{r1}(t)+(r(t)S-2\zeta\omega_0)x_{r2}(t)\\&\quad+\omega_0^2r_s(t))+\hat{r}(t)S\varphi_0(t)+\varphi_2(e_1(t),\hat{e}_2(t))\\&\quad+B_e(e_1(t))(\Theta_1(t)\varphi_1(v(t))+u_p(t))\\&\quad+B_e(e_1(t))\Theta_2(t)\tau(t)\\\hat{e}_2(0)&=\hat{e}_2(\eta_0,v_0,\hat{v}_0,x_{r0}),\quad t\geqslant 0\end{aligned} \tag{48}$$

where

$$\Theta_2(t)\triangleq\begin{bmatrix}\theta_{21}(t)&0\\0&\theta_{22}(t)\\0&\theta_{23}(t)\end{bmatrix},\quad t\geqslant 0 \tag{49}$$

Note that (48) is similar to (21); however, a significant difference is that the uncertain parameters Θ_1^* and Θ_2^* have been replaced by their estimates $\Theta_1(t)$ and $\Theta_2(t)$, $t\geqslant 0$.

The following result presents control laws $\tau(t)$ and $u_p(t)$, $t\geqslant 0$, along with update laws $\dot{\Theta}_1(t)$ and $\dot{\Theta}_{2v}(t)$, $t\geqslant 0$, that will guarantee Lyapunov stability of the error dynamics (14), (45), and (48), as well as convergence of $e_1(t)$, $t\geqslant 0$, to $[a\ \ 0]^{\mathrm{T}}$, in spite of the parametric uncertainties in (2).

Theorem 5.1
Consider the system given by (14), (45), and (48); assume that $B_e(e_1(t))\Theta_2(t)$, $t\geqslant 0$, is non-singular, and that $\beta(0)\neq\pi$. Then, the feedback control laws

$$u_p(e_1,e_v)=B_e^{\mathrm{T}}(e_1)J_s(\beta)\gamma(e_1)+G_ve_v \tag{50}$$

$$\begin{aligned}\tau(t)&=(B_e(e_1(t))\Theta_2(t))^{-1}(-B_e(e_1(t))(\Theta_1(t)\varphi_1(v(t))\\&\quad+u_p(t))-J_s^{\mathrm{T}}(\psi(t))(-\omega_0^2x_{r1}(t)+(r(t)S\\&\quad-2\zeta\omega_0)x_{r2}(t)+\omega_0^2r_s(t))-\varphi_2(e_1(t),e_2(t))\\&\quad-\hat{r}(t)S\varphi_0(\eta(t),v(t),x_r(t))-J_s(\beta(t))\gamma(e_1(t))\\&\quad-G_2\hat{e}_2(t)),\quad t\geqslant 0\end{aligned} \tag{51}$$

along with update laws

$$\dot{\Theta}_1(t)=e_v(t)\varphi_1^{\mathrm{T}}(v(t))\Gamma_1,\quad \Theta_1(t)=\Theta_{10},\quad t\geqslant 0 \tag{52}$$

$$\dot{\Theta}_{2v}(t)=\tau_d(t)e_v(t)\Gamma_2,\quad \Theta_{2v}(t)=\Theta_{2v0} \tag{53}$$

DOI: 10.1002/acs

where $\Gamma_1 \in \mathbb{R}^{10\times 10}$ is a positive-definite matrix and $\Gamma_2 > 0$, guarantee Lyapunov stability of the solution $[e_d(t)\ \beta(t)]^T \equiv [a\ 0]^T$, $\hat{e}_2(t) \equiv 0_{2\times 1}$, $e_v(t) \equiv 0_{3\times 1}$, $\Theta_1(t) \equiv \Theta_1^*$, $\Theta_{2v}(t) \equiv \Theta_{2v}^*$, $t \geqslant 0$, of the dynamics given by (14), (48), (45), (52), and (53). In addition, $(e_d(t), \beta(t)) \to (a, 0)$ and $(e_2(t), e_v(t)) \to (0_{2\times 1}, 0_{3\times 1})$, as $t \to \infty$.

Proof

Substituting the feedback control law (51) into (48), we obtain

$$\dot{\hat{e}}_2(t) = -J_s(\beta(t))\gamma(e_1(t)) - G_2\hat{e}_2(t), \quad t \geqslant 0 \tag{54}$$

Next, consider the Lyapunov function candidate

$$\begin{aligned} V(e_1, \hat{e}_2, e_v, \Theta_1, \Theta_2) &\triangleq e_d \tan^2\left(\frac{\beta}{2}\right) + \frac{1}{2e_d}(e_d - a)^2 + \frac{1}{2}\hat{e}_2^T\hat{e}_2 \\ &\quad + \tfrac{1}{2}\mathrm{tr}[(\Theta_1 - \Theta_1^*)\Gamma_1^{-1}(\Theta_1 - \Theta_1^*)^T] \\ &\quad + \tfrac{1}{2}\mathrm{tr}[(\Theta_{2v} - \Theta_{2v}^*)\Gamma_2^{-1}(\Theta_{2v} - \Theta_{2v}^*)^T] \\ &\quad + \tfrac{1}{2}e_v^Te_v \end{aligned} \tag{55}$$

which is a positive-definite function of $e_d - a$, β, $\hat{e}_2$, e_v, $\Theta_1 - \Theta_1^*$, and $\Theta_{2v} - \Theta_{2v}^*$. The Lyapunov derivative along the closed-loop system trajectories is given by

$$\begin{aligned} \dot{V}(t) &= -e_d(t)\gamma^T(e_1(t))G_1\gamma(e_1(t)) + \gamma^T(e_1(t))J_s^T(\beta(t)) \\ &\quad \times \hat{e}_2(t) - \hat{e}_2^T(t)(J_s(\beta(t))\gamma(e_1(t)) + G_2\hat{e}_2(t)) \\ &\quad + \gamma^T(e_1(t))J_s^T(\beta(t))B_e(e_1(t))e_v(t) \\ &\quad - e_v^T(t)((\Theta_1(t) - \Theta_1^*)\varphi_1(v(t)) + \tau_d(t)(\Theta_{2v}^* \\ &\quad - \Theta_{2v}(t)) + B_e^T(e_1(t))J_s(\beta(t))\gamma(e_1(t)) \\ &\quad + G_ve_v(t)) + \mathrm{tr}[(\Theta_1(t) - \Theta_1^*)\Gamma_1^{-1}\dot{\Theta}_1^T(t)] \\ &\quad + \mathrm{tr}[(\Theta_{2v}(t) - \Theta_{2v}^*)\Gamma_2^{-1}\dot{\Theta}_{2v}^T(t)] \\ &= -e_d(t)\gamma^T(e_1(t))G_1\gamma(e_1(t)) - \hat{e}_2^T(t)G_2\hat{e}_2(t) \\ &\quad - e_v^T(t)G_ve_v(t) - \mathrm{tr}[(\Theta_1(t) - \Theta_1^*)\varphi_1(v(t))e_v^T(t)] \\ &\quad + \mathrm{tr}[(\Theta_1(t) - \Theta_1^*)\Gamma_1^{-1}\dot{\Theta}_1^T(t)] - \mathrm{tr}[(\Theta_{2v}(t) \\ &\quad - \Theta_{2v}^*)e_v^T(t)\tau_d(t)] + \mathrm{tr}[(\Theta_{2v}(t) \\ &\quad - \Theta_{2v}^*)\Gamma_2^{-1}\dot{\Theta}_{2v}^T(t)] \\ &= -e_d(t)\gamma^T(e_1(t))G_1\gamma(e_1(t)) + \mathrm{tr}[(\Theta_1(t) - \Theta_1^*) \\ &\quad \times (\Gamma_1^{-1}\dot{\Theta}_1^T(t) - \varphi_1(v(t))e_v^T(t))] - \hat{e}_2^T(t)G_2\hat{e}_2(t) \\ &\quad - e_v^T(t)G_ve_v(t) + \mathrm{tr}[(\Theta_{2v}(t) - \Theta_{2v}^*)(\Gamma_2^{-1}\dot{\Theta}_{2v}^T(t) \\ &\quad - e_v^T(t)\tau_d(t))], \quad t \geqslant 0 \end{aligned} \tag{56}$$

Substituting update laws (52) and (53) in (56), we obtain

$$\begin{aligned} \dot{V}(t) &= -e_d(t)\gamma^T(e_1(t))G_1\gamma(e_1(t)) - \hat{e}_2^T(t)G_2\hat{e}_2(t) \\ &\quad - e_v^T(t)G_ve_v(t) \leqslant 0 \end{aligned} \tag{57}$$

which according to LaSalle–Yoshizawa's Theorem [14] proves the final statement of the Theorem. □

5.2. Projection algorithm

Note that in (51), the closed form of the command includes the term $(B_e(e_1)\Theta_2)^{-1}$, whose existence was one of the assumptions of Theorem 5.1. To remove this assumption, we will use a projection algorithm [18]. Note that

$$B_e(e_1)\Theta_2 = \begin{bmatrix} -\theta_{21} & -e_d\sin(\beta)\theta_{23} \\ 0 & -\theta_{22} - e_d\cos(\beta)\theta_{23} \end{bmatrix} \tag{58}$$

whose eigenvalues are $-\theta_{21}$ and $-\theta_{22} - e_d\cos(\beta)\theta_{23}$. Following the technique introduced in [18], we define

$$\begin{aligned} f_\lambda(\Theta_{2v}) &= \frac{1}{r_{to}^2 - r_{ti}^2}((\theta_{21} - c_t)^2 + (\theta_{22} - c_t)^2 \\ &\quad + (\theta_{23} - c_t)^2 - r_{ti}^2), \quad t \geqslant 0 \end{aligned} \tag{59}$$

where $c_t > 0$ and $0 < r_{ti} < r_{to}$. We also define the projection operator $P_o(\zeta_0): \mathscr{C}_n \to \mathscr{C}_n$, where $\mathscr{C}_n$ denotes the set of continuous n-valued functions, such that [18]

$$\begin{aligned} P_o(\zeta_0(t)) &\triangleq \zeta_0(t) - \frac{f_\lambda'^T(\Theta_{2v}(t))}{\|f_\lambda'(\Theta_{2v}(t))\|^2}f_\lambda'(\Theta_{2v}(t))\zeta_0(t) \\ &\quad \times f_\lambda(\Theta_{2v}(t)), \quad t \geqslant 0 \end{aligned} \tag{60}$$

DOI: 10.1002/acs

where $f'_\lambda(\Theta_{2v})$ denotes the Fréchet derivative of $f_\lambda(\Theta_{2v})$ with respect to Θ_{2v}. We modify the update law for $\Theta_{2v}(t),\ t\geqslant 0$, as follows [18]:

$$\dot{\Theta}_{2v}(t)=\begin{cases} P_o(\zeta(t)) \text{ if } f_\lambda(\Theta_{2v}(t))\geqslant 0 \text{ and} \\ \qquad\qquad f'_\lambda(\Theta_{2v}(t))\zeta(t)>0 \\ \zeta(t), \qquad \text{otherwise} \end{cases} \tag{61}$$

$$\Theta_{2v}(t)=\Theta_{2v0},\ t\geqslant 0$$

where $\zeta(t)\triangleq\tau_d(t)e_v(t)\Gamma_2,\ t\geqslant 0$. Since the update law (61) only adds a negative term to the Lyapunov derivative (56) [18], the stability properties established in Theorem 5.1 are not modified.

6. NUMERICAL SIMULATION

We will now present results from numerical simulations illustrating the efficacy of the proposed control algorithm. In particular, results using the indirect adaptive algorithm from Section 5 are presented, which show convergence of the trajectory to the reference one, boundedness of the estimates, and behavior of the eigenvalues of $B_e(e_1)\Theta_2$. The control algorithm is used for tracking a circular trajectory and an octomorphic trajectory.

6.1. Circular trajectory

We use the initial estimates $\Theta_{10}=0_{3\times 10}$ and

$$\Theta_{20}=\frac{1}{10}\begin{bmatrix} 1.3 & 0 \\ 0 & -1 \\ 0 & 1 \end{bmatrix} \tag{62}$$

where Θ_{20} is chosen different from $0_{3\times 2}$ to avoid singularity of $B_e(e_1(0))\Theta_{20}$. To accommodate the values of the entries of Θ_2^*, while still being able to force the eigenvalues not to cross zero, we set $c_t=10,\ r_{ti}=c_t-10^{-3},\ r_{to}=c_t-2\times 10^{-3}$. The chosen desired trajectory is circular, of radius 10 m, with a constant traveling speed of 1 m/s. The vehicle's initial position is $\eta_0=[-1\ 0\ 0]^T$ and its initial velocity is zero. The reference trajectory's initial position is chosen slightly off of the vehicle's, to show convergence of the tracking errors, $x_{r10}=[-0.15\ \ -0.6\sqrt{2}]^T$. The gains are chosen as follows: $G_1=10I_2,\ G_2=0.1I_2,\ G_v=10I_3,\ \Gamma_1=0.3I_{10}$, and $\Gamma_2=0.3I_2$. The reference signal is of the form

$$r_s(t)=\omega_0^{-2}(\ddot{x}_d(t)+\omega_0^2 x_d(t)+2\zeta\omega_0\dot{x}_d) \tag{63}$$

where $x_d(t)$ denotes the desired position in the xy-plane at time $t\geqslant 0,\ \zeta=1.2I_2$, and $\omega_0=0.7I_2$. Finally, the constant parameters in $M,\ D(v)$ and $C(v)$, are given by (42), and we choose $a=0.2>a_s$.

The tracking errors converge smoothly to their expected steady-state values. Figure 3 shows that the position error $e_d(t),\ t\geqslant 0$, converges to $a=0.2$, while $\beta(t)$ and $e_2(t),\ t\geqslant 0$, converge to zero. Figure 4 compares the actual and estimated body-fixed velocities, $v(t)$ and $\hat{v}(t),\ t\geqslant 0$. Note that the purpose of the state predictor (43) and update laws (52) and (53) is not necessarily to accurately estimate $v(t),\ t\geqslant 0$, but rather to allow construction of control command (51), in spite of the parametric uncertainties. Nevertheless, Figure 4 shows that the estimated velocities match the actual ones.

Figure 5 shows the trajectory of the actual system (solid curve) converging smoothly to the reference (dashed), which in turn converges to the desired trajectory (dotted). Orientation of the vehicle is represented using black arrows, which demonstrate that the system moves in a coherent fashion. Indeed, the arrows indicate that the vehicle is moving bow first, which is corroborated by the fact that, as seen in Figure 4, the surge velocity $u(t),\ t\geqslant 0$, remains positive throughout the simulation.

Figure 6 shows that the projection algorithm of Section 5 is effective in preventing the eigenvalues of $B_e(e_1(t))\Theta_2(t),\ t\geqslant 0$, from crossing zero, thus ensuring that the inverse of this matrix is well defined. The effects of the projection algorithm are particularly evident for the first eigenvalue, which is constrained away from zero by the projection.

The control input is shown in Figure 7. A saturation technique, similar to that introduced in [20] and extended in [21], was applied to constrain the amplitude of the control effort to reasonable values. Figure 8 shows $\Theta_{2v}(t),\ t\geqslant 0$, and illustrates the boundedness of the estimates.

DOI: 10.1002/acs

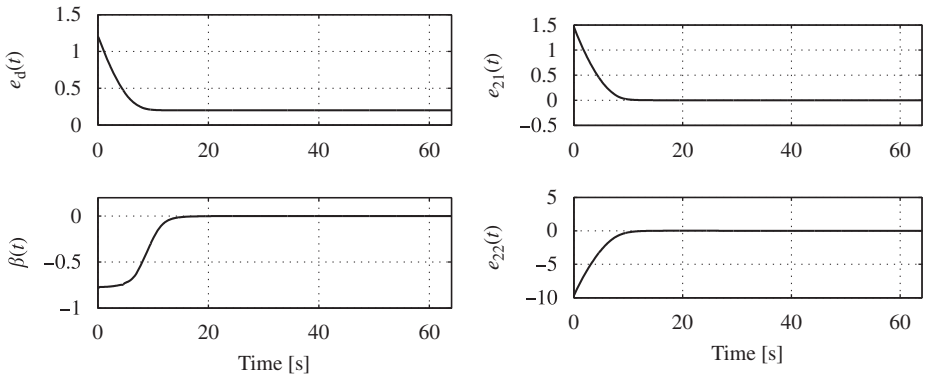

Figure 3. Tracking errors $e_1(t)$ and $e_2(t)$, $t \geqslant 0$, circular trajectory.

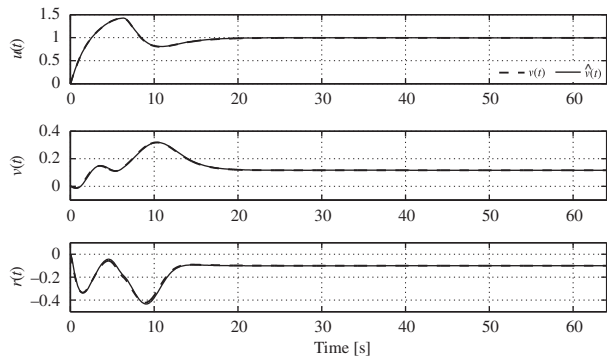

Figure 4. Actual and estimated body-fixed velocities, $v(t)$ and $\hat{v}(t)$, $t \geqslant 0$, circular trajectory.

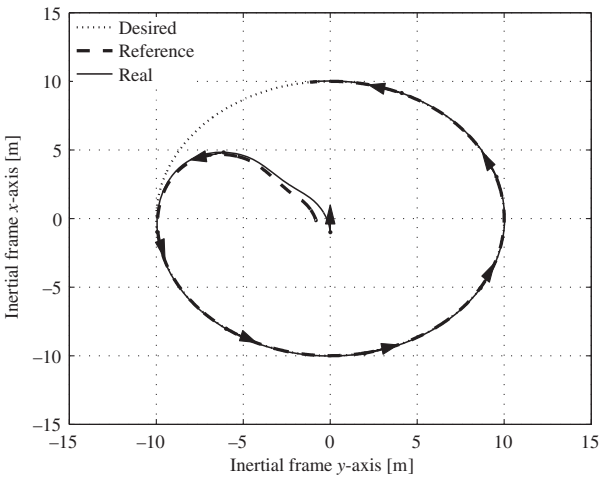

Figure 5. Actual, reference and desired trajectories, circular trajectory.

6.2. *Octomorphic trajectory*

We consider a different desired trajectory, given by

$$x_d(t) = 10[\sin(\omega t) \;\; \sin(\omega t/2)]^T, \quad t \geqslant 0 \qquad (64)$$

with $\omega = 0.1$. The initial position is $\eta_0 = [-1 \;\; 0 \;\; 0]^T$, while the initial reference position is $x_{r10} = [0.2 \;\; 0]^T$. All other initial conditions, gains, and parameters remain identical to what was chosen for the previous example.

As shown in Figure 9, the behavior is similar to that observed with a circular desired trajectory. The vehicle converges smoothly to the desired trajectory, and the orientation, still indicated by black arrows, remains appropriate. The control command can be found in Figure 10 and the estimate $\Theta_{2v}(t)$, $t \geqslant 0$, in Figure 11.

7. CONCLUSIONS

The presented results address trajectory tracking in the horizontal plane for marine vehicles equipped with a fixed thruster and a rudder or, equivalently, a vectored thruster. Such vehicles are characterized by

DOI: 10.1002/acs

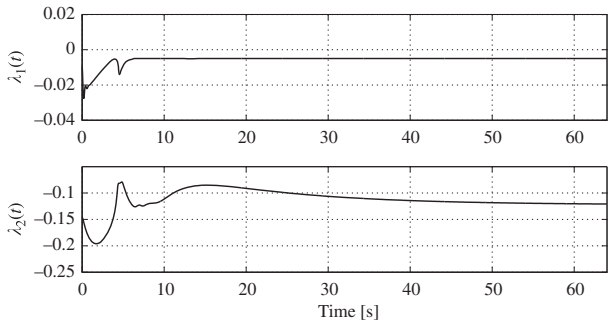

Figure 6. Eigenvalues of $B_e(e_1(t))\Theta_2(t)$, $t \geqslant 0$, circular trajectory.

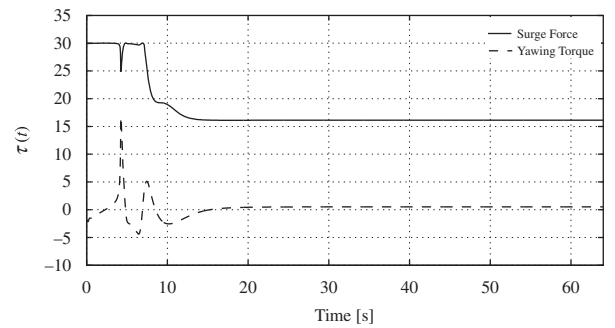

Figure 7. Control command $\tau(t)$, $t \geqslant 0$, circular trajectory.

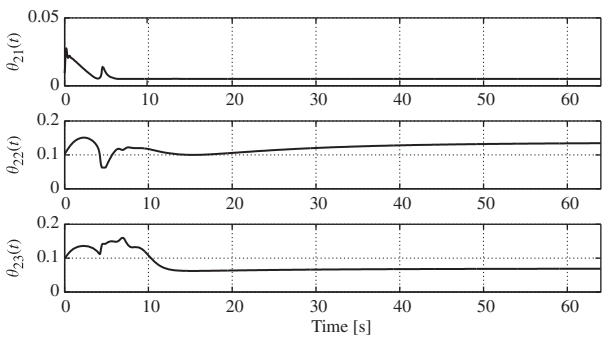

Figure 8. Elements of the parameter estimate vector $\Theta_{2v}(t)$, $t \geqslant 0$, circular trajectory.

a non-minimum phase-type behavior. To overcome the unstable nature of the system's internal dynamics, special tracking errors were selected. First, a control

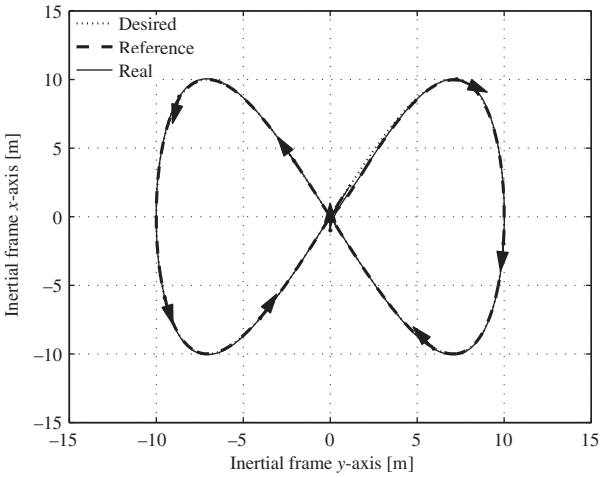

Figure 9. Actual, reference and desired trajectories, octomorphic trajectory.

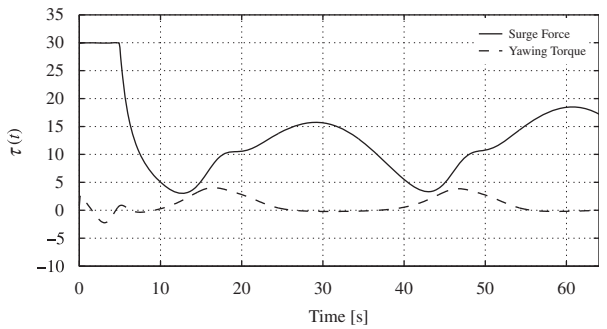

Figure 10. Control command $\tau(t)$, $t \geqslant 0$, octomorphic trajectory.

algorithm that assumes knowledge of the parametric uncertainties in the model was presented, which guarantees global asymptotic stability of the tracking errors. Then, the impact of the chosen control strategy on the internal dynamics was assessed. It was shown that the proposed control framework, through design of a constant design parameter, guarantees local stability of the zero-dynamics for a simple maneuver. Finally, since the obtained control law depends on uncertain parameters, an adaptive control algorithm was derived. Furthermore, the unknown parameters appear nonlinearly in the command; hence, an indirect adaptive technique was chosen instead of the more commonly

DOI: 10.1002/acs

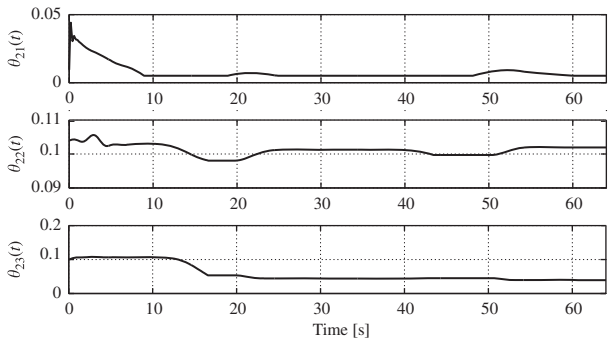

Figure 11. Elements of the parameter estimate vector $\Theta_{2v}(t),\ t \geqslant 0$, octomorphic trajectory.

found direct adaptive procedures. The obtained adaptive control algorithm guarantees convergence of the tracking errors and Lyapunov stability of the dynamics, in spite of the parametric uncertainties. Numerical simulations illustrate the excellent performance of the indirect adaptive control algorithm in the case of circular and octomorphic trajectories. In addition, the results from the simulations correlate with our stability analysis of the zero-dynamics, as they show the vehicle moving bow first, meaning that the system's velocity in surge remains positive.

REFERENCES

1. Encarnação P, Pascoal A. Combined trajectory tracking and path following: an application to the coordinated control of autonomous marine craft. *Proceedings of the 40th IEEE Conference on Decision and Control*, vol. 1, Orlando, FL, 2001; 964–969.
2. Dougherty F, Sherman T, Woolweaver G, Lovell G. An autonomous underwater vehicle (AUV) flight control system using sliding mode control. *Proceedings of the OCEANS'88 Conference*, Baltimore, MD, 1988; 1265–1270.
3. Fjellstad OE, Fossen TI. Position and attitude tracking of AUV's: a quaternion feedback approach. *IEEE Journal of Oceanic Engineering* 1994; **19**:512–518.
4. Lainiotis D, Menon D, Plataniotis K, Charalampous C. Adaptive filter applications to autonomous underwater vehicle. *Proceedings of the OCEANS'93 Conference*, vol. 2, Victoria, Canada, 1993; 295–300.
5. Toussaint G, Basar T, Bullo F. Tracking for nonlinear underactuated surface vessels with generalized forces. *Proceedings of the International Conference on Control Application*, Anchorage, AK, 2000; 355–360.
6. Toussaint G, Basar T, Bullo F. H^{∞}-optimal tracking control techniques for nonlinear underactuated systems. *Proceedings of the 39th IEEE Conference on Decision and Control*, vol. 3, Sydney, Australia, 2000; 2078–2083.
7. Encarnacão PMM. Nonlinear path following control systems for ocean vehicles. *Ph.D. Thesis*, Instituto Superior Technico, 2002.
8. Fossen TI, Godhavn JM, Berge SP, Lindegaard KP. Nonlinear control of underactuated ships with forward speed compensation. *Proceedings of the IFAC NOLCOS98*, vol. 1, Enschede, Netherlands, 1998; 121–126.
9. Godhavn J-M. Nonlinear control of underactuated surface vessels. *Proceedings of the 35th IEEE Conference on Decision and Control*, vol. 1, Kobe, Japan, 1996; 975–980.
10. Aguiar A, Pascoal A. Regulation of a nonholonomic autonomous underwater vehicle with parametric modeling uncertainty using Lyapunov functions. *Proceedings of the 40th IEEE Conference on Decision and Control*, Orlando, FL, 2001; 4178–4183.
11. Fredriksen E, Pettersen KY. Global κ-exponential way-point manoeuvering of ships. *Proceedings of the 43rd IEEE Conference on Decision and Control*, Paradise Island, Bahamas, 2004; 5360–5367.
12. Breivik M, Fossen TI. A unified control concept for autonomous underwater vehicles. *Proceedings of the American Control Conference*, Minneapolis, MN, June 2006; 4920–4926.
13. Leonessa A, Van Zwieten TS, Morel Y. Neural network model reference adaptive control of marine vehicles. *Current Trends in Nonlinear Systems and Control*. Birkhäuser: Basel, 2004.
14. Krstić M, Kanellakopoullos I, Kokotović P. *Nonlinear and Adaptive Control Design*. Wiley: New York, NY, 1995.
15. Swaroop D, Hedrick J-K, Yip P-P, Gerdes J-C. Dynamic surface control for a class of nonlinear systems. *IEEE Transactions on Automatic Control* 2000; **45**:1893–1899,
16. Morel Y. Design of an adaptive nonlinear controller for an autonomous underwater vehicle equipped with a vectored thruster. *Master Thesis*, Florida Atlantic University, 2002.
17. Hovakimyan N, Lavretsky E, Cao C. Adaptive dynamic inversion via time-scale separation. *Proceedings of the 45th IEEE Conference on Decision and Control*, San Diego, CA, 2006.
18. Pomet JB, Praly L. Adaptive nonlinear regulation: estimation from the Lyapunov equation. *IEEE Transactions on Automatic Control* 1992; **37**:729–740.
19. Fossen TL. *Guidance and Control of Ocean Vehicles*. Wiley: Chichester, England, 1999.
20. Leonessa A, Haddad WM, Hayakawa T. Adaptive control for nonlinear uncertain systems with actuator amplitude and rate saturation constraints. *American Control Conference*, Arlington, VA, 2000.
21. Leonessa A, Haddad WM, Hayakawa T, Morel Y. Adaptive control for nonlinear uncertain systems with actuator amplitude and rate saturation constraints. *International Journal of Adaptive Control and Signal Processing* 2009; **23**(1):73–96.

DOI: 10.1002/acs